

Underwater acoustic impacts of shipping management measures: Results from a social-ecological model of boat and whale movements in the St. Lawrence River Estuary (Canada)



Clément Chion ^{a,*}, Dominic Lagrois ^a, Jérôme Dupras ^a, Samuel Turgeon ^b, Ian H. McQuinn ^c, Robert Michaud ^d, Nadia Ménard ^b, Lael Parrott ^e

^a Department of Natural Sciences, Université du Québec en Outaouais, Canada

^b Saguenay-St. Lawrence Marine Park, Parks Canada, Canada

^c Institut Maurice-Lamontagne, Fisheries and Oceans Canada, Canada

^d Group for Research and Education on Marine Mammals, Canada

^e Departments of Earth, Environmental and Geographical Sciences and Biology, University of British Columbia (Okanagan), Canada

ARTICLE INFO

Article history:

Received 17 October 2016

Received in revised form 16 March 2017

Accepted 17 March 2017

Available online 1 April 2017

Keywords:

Agent-based model
Endangered species conservation
Marine protected area
Human-wildlife interactions
Underwater acoustic impact assessments
Whale ecology
Acoustic modelling
Noise in the environment
Individual-based model
Coupled human-natural system

ABSTRACT

The recovery of whale species at risk requires the implementation of protection measures designed to mitigate the risks posed by various stressors. In the St. Lawrence Estuary (Canada), several whale species are threatened by navigation activities in various ways. Since 2013, seasonal voluntary ship strike mitigation measures, including a speed reduction area (SRA) and a no-go area, were implemented annually and largely adopted by the maritime industry to reduce the risks of lethal collisions with four species of baleen whales. While the endangered St. Lawrence beluga population is unlikely to be subject to collisions with large merchant ships, it is known to be negatively affected by vessel-generated underwater noise. To assess how these protection measures modify the beluga's soundscape throughout their critical habitat, we implemented an underwater acoustic module within an existing agent-based model (3MTSim) of ship-whale movements and interactions in the St. Lawrence Estuary. We ran multiple simulations for two scenarios 1) without and 2) with the protection measures to compare the level of noise received by belugas before and after 2013. Overall, the simulations showed a statistically-significant 1.6% decrease in the total amount of noise received by belugas in their critical habitat following the implementation of the protection measures. Although slowing down ships reduces instantaneous radiated noise, it also increases the total amount of acoustic energy released in the environment by extending the time spent in the SRA. Accordingly, our simulations showed a 2.4% increase in the cumulative noise from shipping received by beluga in the SRA. Conversely, belugas located in the Upper Estuary, mostly females and calves, i.e., the most valuable individuals experienced a 5.4% reduction in the cumulative received level of shipping noise. Although refinements are required to improve the modelling of noise sources and propagation for finer scale projections in this complex nearshore environment, this agent-based modelling paradigm of 3MTSim proved informative for underwater acoustic impact assessments.

Crown Copyright © 2017 Published by Elsevier B.V. All rights reserved.

1. Introduction

The St. Lawrence River Estuary (SLE) in Canada is an important habitat for marine mammals year round, although mainly from May to October. Among them, the resident St. Lawrence beluga whale population (*Delphinapterus leucas*) along with the migratory Northwest Atlantic blue whale (*Balaenoptera musculus*) and the Atlantic

fin whale population (*Balaenoptera physalus*) are listed under the Canadian Species At Risk Act (*Species at Risk Act (Canada), 2002*). Two other baleen whale species along with several species of seals and odontocetes are also frequent visitors of the SLE during summertime, mainly for foraging purposes (*Michaud et al., 1997a*).

In addition to its rich biodiversity, the SLE is a major seaway linking the Atlantic Ocean to the Great Lakes. Each year, merchant ships conduct more than 7000 transits through the SLE to which are added thousands of trips by whale-watching boats, ferries and pleasure craft (*Chion et al., 2009*). The resulting co-occurrences between boats and whales have raised concerns about negative

* Corresponding author.

E-mail address: clementchion@gmail.com (C. Chion).

impacts including both collisions and exposure to underwater noise. While the negative impacts of collisions are obvious, underwater noise impacts on whales such as belugas include behavioral changes affecting foraging efficiency, e.g. avoidance and disturbance (Gomez et al., 2016), changes in vocalizing behaviour (Lesage et al., 1999), communication masking affecting an animal's ability to socialize and locate prey (Erbe et al., 2016) and hearing loss (Finneran et al., 2002; Schlundt et al., 2000). In the SLE, such threats are identified as potentially limiting the recovery of the North Atlantic blue whale (Beauchamp et al., 2009) and the St. Lawrence beluga population (Fisheries and Oceans Canada, 2012). Although avoidance behaviors have been observed in the study area, we know very little about frequency-dependent thresholds of noise levels that trigger such responses with potential long-term consequences (Gomez et al., 2016). Similarly, other potentially critical impacts of anthropogenic noise on belugas including the masking of their vital acoustic activities, e.g. echolocation, communication (Erbe et al., 2016) remain unclear at present.

The Saguenay-St. Lawrence Marine Park (marine park thereafter) is a marine protected area co-managed by Parks Canada and Parcs Québec located at the heart of the St. Lawrence beluga's critical habitat (Fisheries and Oceans Canada, 2012; Government of Canada, 1997). The marine park was initially designed to enhance the conservation of marine mammals with particular reference to the endangered beluga whale (cf. Fig. 1) and its regulations have been mainly designed with regard to managing the commercial and recreational whale-watching industry (Parks Canada, 2002). However, the issue of the risks of lethal ship strikes by merchant ships on large whales was not addressed by these regulations. Therefore, an interdisciplinary research project was initiated in 2006 to build decision support tools to inform the mitigation of ship-whale collisions in the SLE (Parrott et al., 2011). Following two years of collaboration, the Working Group for Maritime Transportation and Marine Mammal Protection (Working Group thereafter) involving stakeholders from the public, private, NGO, and academic sectors recommended in 2013 a set of voluntary protection measures to enhance marine mammal protection and considered compliance would not require mandatory regulations (Canadian Coast Guard, 2016). As it was determined that the risks of lethal collisions to large marine mammals increased with ship speed and the number of ship-whale co-occurrences (Laist et al., 2001; Vanderlaan and Taggart, 2007), the protection measures include a Speed Reduction Area (SRA), a No-Go Area (NGA), and a recommendation to navigate in the northern part of the SLE to keep transiting ships away from the south shore highly used by pods of female and young belugas (Fig. 1). These measures are intended to reduce the risks of lethal collisions between merchant ships and baleen whales without increasing the level of noise exposure for belugas (Parrott et al., 2016).

More than 3 years after the implementation of the protection measures in the SLE, the risks of lethal collisions between large merchant ships and the five main species of baleen whales have decreased by up to 40% in the marine park from May to October (Chion, 2016). These gains in conservation are mostly due to the maritime industry's compliance with the voluntary SRA (Parrott et al., 2016), as shown in the Fig. A1d (Appendix A). For the Saguenay River and the Upper Estuary, no statistically-significant change in average ship speed was found after as compared to before the implementation of the protection measures (cf. Fig. A1a and b), confirming the absence of side-effects beyond their spatial boundaries.

These protection measures were intended to mitigate the risks of collision between large merchant ships and baleen whales in the SLE where these species mostly concentrate (Chion et al., 2012; Michaud et al., 1997b, 2008; Michaud and Giard, 1997). Beluga whales are considered subject to collisions with highly maneuverable and fast-moving boats (Fisheries and Oceans Canada, 2012)

however, large merchant ships do not appear to be involved in mortality events attributed to ship strikes. This is possibly because collisions with large vessels are likely to result in a complete sectioning of the body, although this has not been documented (Lair et al., 2016). Nonetheless, the beluga is a toothed whale relying heavily on sound to communicate, as well as to locate and hunt their prey (Erbe et al., 2016; Lesage et al., 1999; Weilgart, 2007). By modifying some shipping-traffic parameters (mostly speed), compliance with the protection measures may have inadvertently modified the beluga's soundscape. Given the absence of any permanent acoustic monitoring system throughout the beluga's critical habitat, we proposed to combine agent-based modelling with acoustic sound-source and propagation models to assess the likely changes induced by the collision protection measures to the beluga's summer-habitat soundscape.

In the context of the Working Group's adaptive management process, our objectives were to assess the likely acoustic impacts of the voluntary protection measures on the SLE beluga's soundscape and to recommend further actions to investigate this emerging issue of the effects of anthropogenic noise. To this end, we report on the simulation results of a new version of the Marine Mammals and Maritime Traffic Simulator (3MTSim), an agent-based spatial model of boat and whale movements (Parrott et al., 2011) which has already been used to support management decisions in the SLE (Chion et al., 2012, 2013). This revised version of 3MTSim integrates acoustic models of both sound sources (i.e. merchant ships) and underwater noise propagation (i.e. transmission loss) to simulate the soundscape under various marine traffic scenarios. We first give an overview of 3MTSim described in previous publications (Chion, 2011; Chion et al., 2011; Lamontagne, 2009; Parrott et al., 2011) followed by a description of the acoustic models including the data used for calibration. We further present 3MTSim simulation results focusing on the changes in the beluga's soundscape with and without the ship-strike mitigation measures to detect any potential positive or negative side-effects. After a discussion of our results with regard to the known ecological characteristics of the beluga population, we conclude with some management implications of our results and identify future work to refine 3MTSim as an acoustic impact assessment tool.

2. Materials and methods

2.1. 3MTSim general overview

Relying on more than 25 years of data collection on whale ecology and the recent availability of data on navigation activities in the SLE and the Saguenay River (cf. map), 3MTSim was implemented using the agent-based modelling paradigm (Bonabeau, 2002; Grimm et al., 2005). 3MTSim simulates the movements of individual boats (2D) and marine mammals (3D) through the study area (cf. Fig. 1) at 1-min time intervals (Parrott et al., 2011). The primary goal of this social-ecological model is to assess how alternative scenarios of traffic management in the study area would potentially impact both marine mammals and navigation activities. The main indicators returned by the first version of 3MTSim were the transit times across the area for merchant ships, the activity budget for whale-watching vessels, the frequency of encounters between marine mammals and boats, and the risks of lethal ship strikes (see (Parrott et al., 2011) for a full description of the simulator and data). After several validation steps (Chion, 2011; Chion et al., 2011; Lamontagne, 2009), 3MTSim was used to inform various policy-making processes mostly related to the reduction of boat-whale close encounters (Chion et al., 2014, 2013) and the mitigation of ship strike risks (Chion et al., 2012).

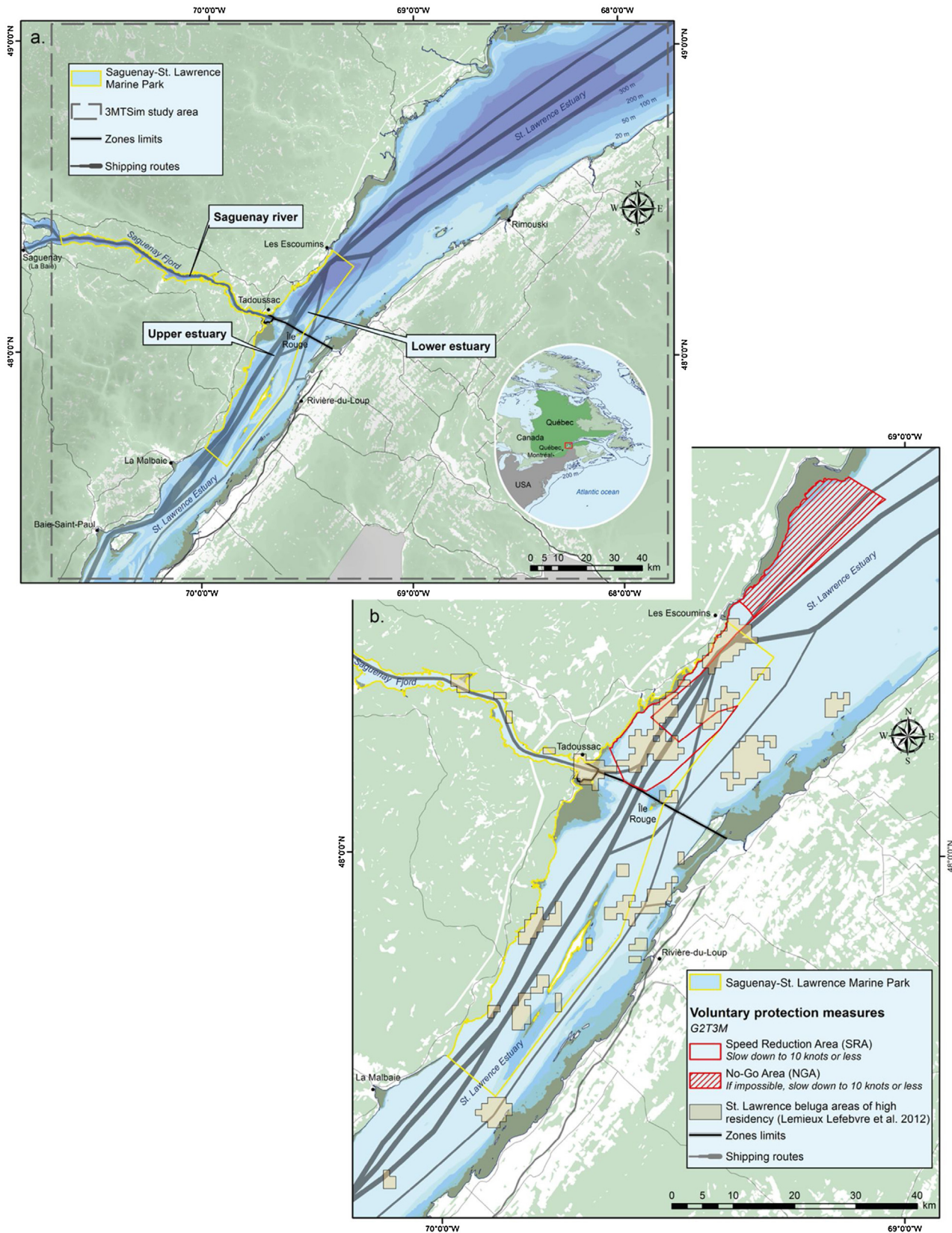


Fig. 1. (a) Study area; (b) Zoom on the protection measures showing belugas' high residence areas.

To include the acoustic dimension within 3MTSim, we relied on observational data of ship sound signatures (*i.e.* acoustic source model thereafter) collected using several hydrophones

along with noise propagation model parameters (*i.e.* propagation/transmission loss model thereafter) measured throughout the study area (for hydrophone locations, see (McQuinn et al., 2011)).

Table 1
Vessel Properties.

Name	Class	<i>l</i> (m)	<i>v</i> (kts)	<i>K</i> ₀ (dB re 1 μPa/√Hz @ 1 m)
Algoisle	Bulk Carrier	223	16.5	-13.5
CSL Assiniboine	Bulk Carrier	224	10.8	-4.5
Cap Romuald	Crude Oil Tanker	274	10.5	-5.1
Cherkassy	General Cargo	177	14.3	-8.0
Federal Yoshino	Bulk Carrier	190	12.7	-5.4
Kemeri	Oil/Chemical Tanker	152	11.0	-6.2
Maersk Perth	Container	211	19.5	-18.4
Pomorze Zachodnie	Bulk Carrier	180	13.6	-11.7
Team Leopard	Chemical Tanker	172	15.3	-7.7
Valgogen	Bulk Carrier	223	12.3	-0.6
CP Venture	Container	294	15.6	-7.0

These data and parameters were made available by the Department of Fisheries and Oceans Canada (Lesage et al., 2014; McQuinn et al., 2011). Therefore, in 3MTSim each ship is considered a point-source emitting an isotropic noise field, which is a valid assumption for far-field measurements (ANSI, 2009). At each time step of a simulation, the total amount of noise received by the simulated whales is equal to the sum (in the linear domain) of the transmitted noise from all contributing ships in their direct line of sight (*i.e.* no obstacle between the ship and the whale in 3D). Both the acoustic source and the propagation/transmission loss models are described in the following sections.

2.2. Acoustic source model

The acoustic subroutine treats each ship as a singular point-source emitting noise isotropically. Source spectra were numerically synthesized according to the Research Ambient Noise DIrectionality model (hereafter referred as RANDI, (Breeding et al., 1996)) that provides source levels in the frequency domain computed from the targeted ship length (*l*) and speed (*v*). The source spectral density levels *L_S*, expressed in units of dB re 1 μPa/√Hz @ 1m, were provided by:

$$L_S(f, v, l) = L_{SO}(f) + 60\log_{10}\left(\frac{v}{v_0}\right) + 20\log_{10}\left(\frac{l}{l_0}\right) + df \times dl \quad (1)$$

where *l* and *v* were expressed in units of feet and knots, respectively while reference length *l*₀ and speed *v*₀ were fixed at 300 feet and 12 knots.

The original studies (see, e.g., (Ross, 1987)) estimated the *L_{SO}(f)* term as:

$$L_{SO}(f) = -10\log_{10}\left(10^{-1.06\log_{10}(f)-14.34} + 10^{3.32\log_{10}(f)-21.425}\right) \quad \begin{array}{ll} \text{if } f \leq 500 \text{ Hz} \\ = 173.2 - 18.0\log_{10}(f) \quad \text{if } f > 500 \text{ Hz} \end{array} \quad (2)$$

where the frequency *f* is expressed in units of Hz. The far-right terms *df* and *dl* in Eq. (1) were fixed at:

$$\begin{aligned} df &= 8.1 & \text{if } f \leq 2.84 \text{ Hz} \\ &= 22.3 - 9.77\log_{10}(f) & \text{if } f > 2.84 \text{ Hz} \end{aligned} \quad (3)$$

and,

$$dl = \frac{l^{1.15}}{3643.0} \quad (4)$$

Recent observations of large vessels (*l*>150 m) have shown that the RANDI predictions substantially overestimate measured source levels (Erbe et al., 2012; McKenna et al., 2012). This could be attributed to the important decrease in cavitation effects (*e.g.*, higher maintenance standards, more efficient blades/engine designs) that took place since the empirical development of the RANDI equations a few decades ago. To examine the precision of Eqs. (1)–(4), field observations obtained from large vessels in the SLE, during the summers of 2004–2005, were used (Lesage et al.,

2014; McQuinn et al., 2011). Spectral signatures and source levels for 11 ships, between 0.02 and 20 kHz, were available to assess the discrepancy between the RANDI model in its actual form and source levels retrieved from modern vessels transiting in our area of interest. The name, length and speed for each ship are listed in Table 1.

The preliminary plots using the original RANDI model all showed an excess of the theoretical model predictions when compared to the observational data (cf. dashed line in Fig. 3). Below 2000 Hz, this excess is constant (*i.e.*, frequency-independent), estimated between approximately 1 and 20 dB re 1 μPa/√Hz @ 1m depending on the targeted ship. This indicates that the original RANDI model, although predicting source levels consistently greater than observations, could appropriately reproduce the shape of the hydrophone-assisted spectra in the dominant low-frequency domain. Above 2000 Hz, the RANDI model's overestimation increases monotonically at intermediate and high frequencies. This steep model overshoot is likely accurate, since the more pronounced decreasing slope above 2000 Hz was observed for almost all 11 targets. We note that the authors carefully addressed molecular absorption at high frequencies during data reduction. This leads to our first modification of the original RANDI model. In order to maintain RANDI's excess constant in all frequency regimes, Eq. (2) was re-processed according to:

$$\begin{aligned} L_{SO}(f) &= -10\log_{10}\left(10^{-1.06\log_{10}(f)-14.34} + 10^{3.32\log_{10}(f)-21.425}\right) & \text{if } f \leq 500 \text{ Hz} \\ &= 173.2 - 18.0\log_{10}(f) & \text{if } 500 < f < 2000 \text{ Hz} \\ &= 219.2 - 32.0\log_{10}(f) & \text{if } f > 2000 \text{ Hz} \end{aligned} \quad (5)$$

with the addition of a third term to the original equations. This additional term minimizes the residuals obtained from the subtraction of the theoretical and observed data. Following the replacement of Eq. (2) by Eq. (5), the discrepancy between the RANDI model and the hydrophone-based data was now roughly constant at all frequencies. Eq. (1) was therefore modified as follows:

$$L_S(f, v, l) = L_{SO}(f) + 60\log_{10}\left(\frac{v}{v_0}\right) + 20\log_{10}\left(\frac{l}{l_0}\right) + df \times dl + K_0 \quad (6)$$

where the right-hand term *K*₀ is a vessel-dependent constant with units of dB re 1 μPa/√Hz @ 1m and is treated as a free parameter. For each ship, this *K*₀ parameter was fitted to minimize the mean residual across the frequency band between 0.02 and 20 kHz. Since the RANDI model constantly overestimates the observed source levels, *K*₀ is always negative (Table 1). No specific correlation was established between *K*₀ and the length *l* of each vessel. However, the magnitude of *K*₀ appears to increase with *v*. The regression shows a Pearson correlation coefficient of (-)0.82 hence suggesting that *K*₀ ≈ *K*₀(*v*). Regrouping the speed-dependent terms from Eq. (6) yields:

$$60\log_{10}\left(\frac{v}{v_0}\right) + K_0(v) = K_0(v)\log_{10}\left(\frac{v}{v_0}\right) \quad (7)$$

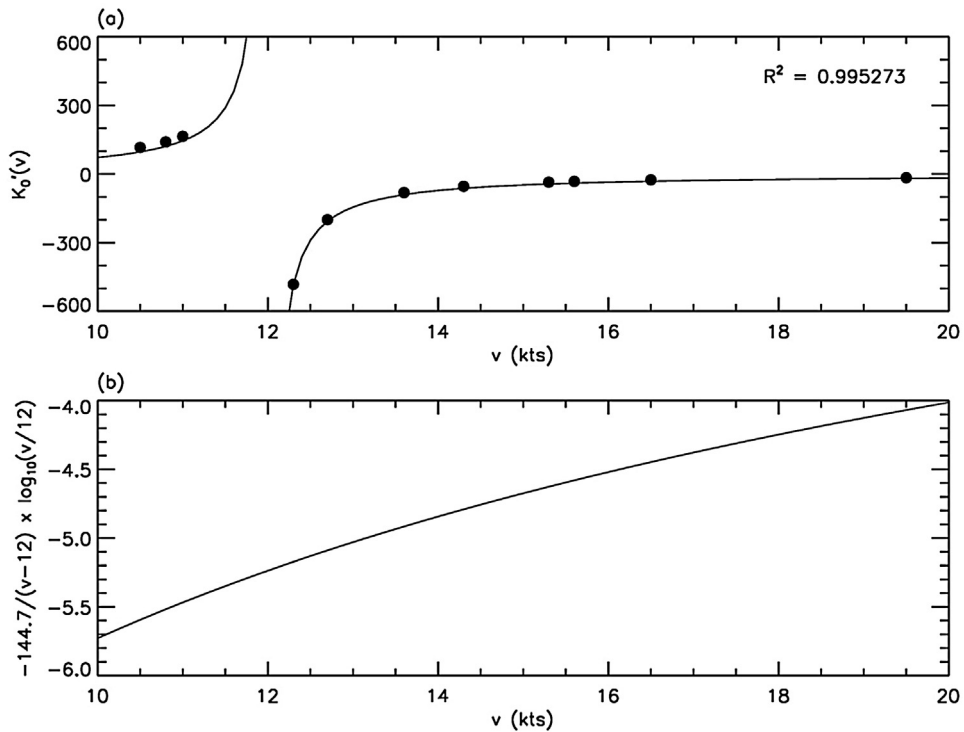


Fig. 2. Panel (a). Point-plot diagram of the $K_0(v)$ parameter, shown as filled circles, with respect to v for all targets listed in Table 1 [see Eq. (7)]. The data points were fitted using an inverse function shown as the thick, solid line. Panel (b). Behavior with v of the speed-dependent term in our renormalization of the RANDI equation [see Eq. (9)].

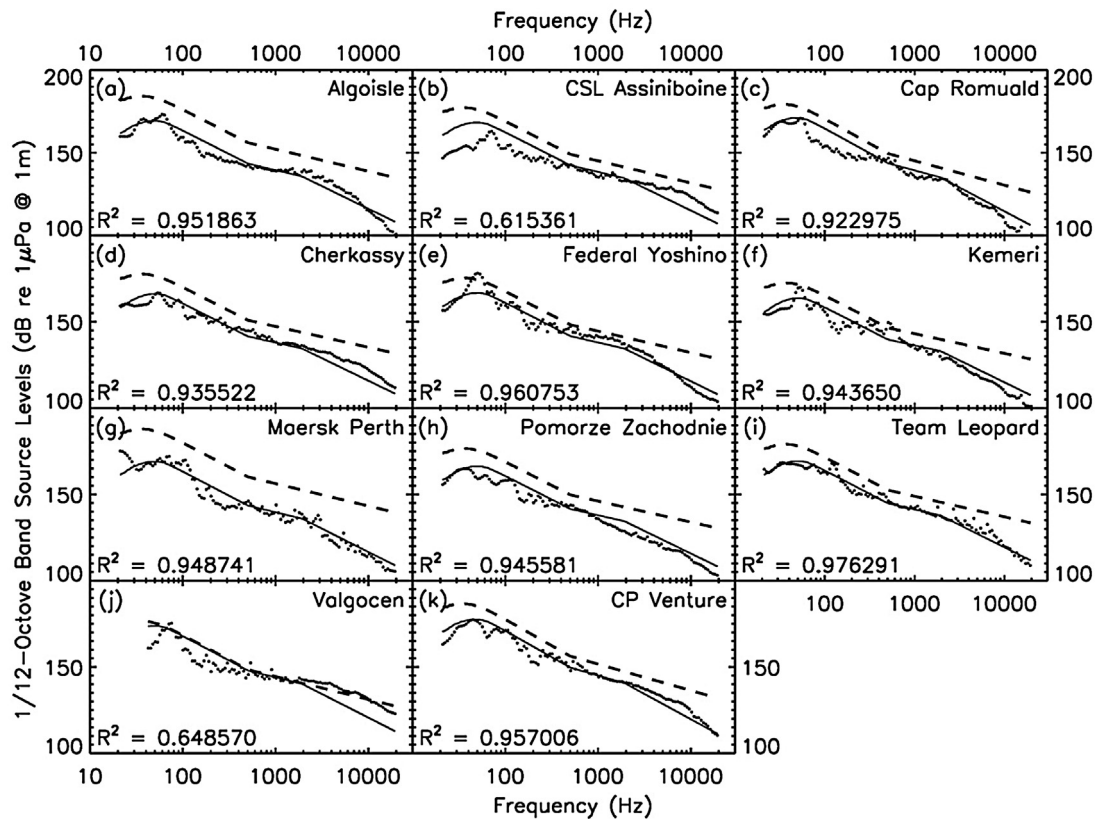


Fig. 3. Black dots: 1/12-octave band source levels provided for 11 large vessels transiting in the St. Lawrence Estuary (Lesage et al., 2014; McQuinn et al., 2011). Dash lines: Synthesized spectra obtained from the original RANDI model (Breeding et al., 1996). Solid lines: Synthesized spectra obtained from Eq. (9) provided each ship length and speed (see Table 1).

From each $v \cdot K_0(v)$ pair retrieved from Table 1 and using Eq. (7), the $K'_0(v)$ parameter was computed and then displayed for each vessel in Fig. 2a with respect to v . The curve perfectly agrees with that of a standard inverse function with asymptotic behavior centered at $v = v_0 = 12$ knots. The $v \cdot K'_0(v)$ relation was then fitted to:

$$K'_{0,fit}(v) = \frac{-144.7}{v - 12} \quad (8)$$

Finally, Eqs. (7) and (8) are substituted in Eq. (6) leading to a renormalization of the RANDI model according to:

$$L_S(f, v, l) = L_{S0}(f) - \frac{144.7}{v - 12} \log_{10}\left(\frac{v}{v_0}\right) + 20 \log_{10}\left(\frac{l}{l_0}\right) + df \times dl \quad (9)$$

Fig. 2b shows how the speed-dependent term (i.e., the second term in Eq. (9)) behaves with v . The monotonically increasing trend agrees with the original RANDI theory suggesting that the source spectral density levels should increase with increasing v . The limit theorem was used to estimate the value in ordinates as v approaches 12 knots.

Fig. 3 illustrates how Eq. (9), using the length and speed values of Table 1, fits the observed source spectra provided by our set of 11 ships. Except for poorer fits in Panels (b) and (j), the results were judged satisfactory with R^2 greater than 0.92 (Fig. 3). In order to examine the statistical reliability of Eq. (9) on larger groups, a series of vessel transits waypoints recorded from 2002 to 2006 in the marine park by the Canadian Coast Guard (INNAV system) were obtained. Length, speed, and class are provided for each ship. Events for vessel classes specifically modeled by the 3MTSim simulator were extracted. From Eq. (9), the broadband source levels between 0.01 and 160 kHz for 40 bulk carriers, 28 tankers, 17 vehicle carriers, 33 cargo ships, and 21 container ships were computed.

Considering the good match between source data and the adjusted RANDI model (Fig. 3), Eqs. (3)–(5), and (9) of this subsection were chosen to synthesize source-level spectra in 3MTSim.

Whisker plots (Fig. 4) display the range in source levels covered by each vessel class of the marine park dataset. For comparison, broadband measurements from other studies were added to the diagram. Our results match relatively well those from other authors giving support to our re-calibration of the original RANDI model.

2.3. Propagation/transmission loss model

To account for the acoustic energy loss while sound propagates from sources (ships) to receivers (belugas), we implemented an acoustic transmission loss model within 3MTSim. At each timestep τ_i of a given run of 3MTSim, the source-level spectrum in the frequency domain of each source present in the computational volume was computed in 1/3-octave bands between 0.01 and 160 kHz. Each band was then isotropically transmitted in the simulated underwater medium surrounding the source's position. Received levels of sound were computed at the positions of marine mammals in the path of the propagation. Alternatively, the sound was assumed to be fully absorbed if it encountered an obstacle e.g., an island located along a transect connecting a ship and a marine mammal. Sound propagation was solved using the standard SONAR equation:

$$SL(f, r_0) = RL(f, r) + TL(r_0|r) + TL_{abs}(f, r_0|r) \quad (10)$$

where the source level $SL(f, r_0)$, for frequency f at the source's position r_0 , and the received level $RL(f, r)$, for frequency f at the receiver's position r , are linked by the transmission loss $TL(r_0|r)$, quantitatively describing the spatial attenuation of the sound as it travels away from the source between r_0 and r , and the frequency-dependent absorption caused by water molecules $TL_{abs}(f, r_0|r)$ also sustained between r_0 and r .

Following the work of McQuinn et al. (2011) geometrical spreading was used to quantify $TL(r_0|r)$ according to:

$$TL(r_0|r) = \beta \cdot \log_{10}\left(\frac{r - r_0}{1 \text{ m}}\right) \quad (11)$$

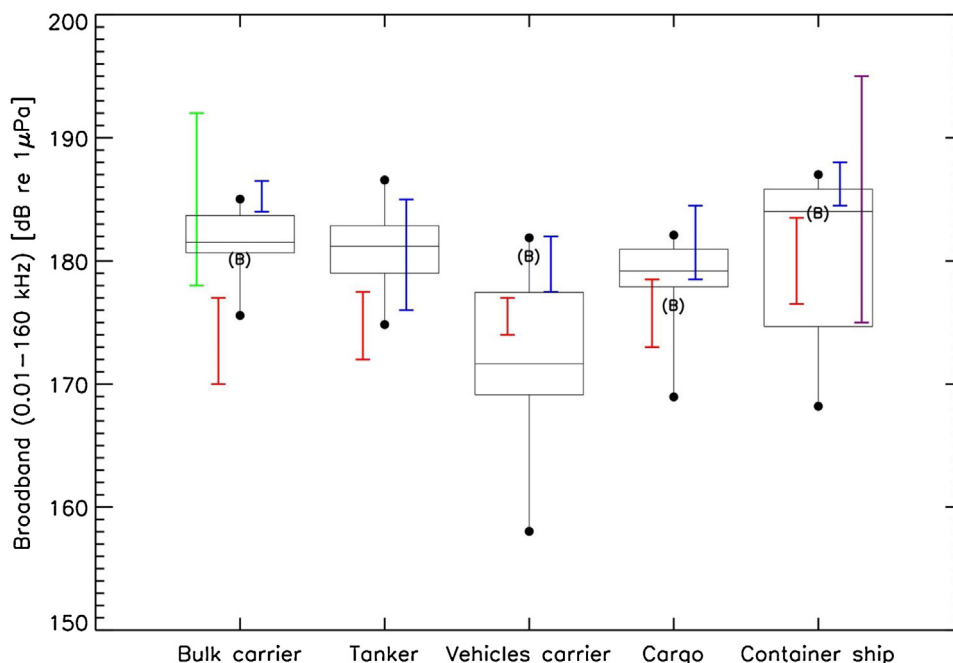


Fig. 4. Broadband source levels, between 0.01 and 160 kHz, obtained from the marine park dataset of transiting vessels in the St. Lawrence Estuary and the re-normalization of the RANDI model in Eq. (9). Whisker plots are drawn for each class using 1, 25, 50, 75, and 99% percentiles. Minimal and maximal values for each distribution are shown as filled circles. Each (B) symbol represents the mean obtained by Bassett et al. (2012). Blue bars are means from McKenna et al. (2012). The purple bar corresponds to an estimate for container ships provided by McKenna et al. (2013) while the green bar is an estimate by Arveson and Vendittis (2000). Red bars enclose the 25-to-75% percentiles provided by Veirs et al. (2016). (For interpretation of the references to colour in this figure legend, the reader is referred to the web version of this article.)

Data sources: Canadian Coast Guard INNAV system.

Table 2

3MTSim parameters (inputs).

Parameter	Description	Value range (unit)	Comments and references
S	Water salinity	35 (%)	Erbe et al. (2012)
T	Water temperature	10 (°C)	Erbe et al. (2012)
pH	Water pH	8	Erbe et al. (2012)
z	Depth	[0–350] (m)	Bathymetric map
$\alpha(f)$	Absorption coefficient	Given by Eq. (13) (dB re 1 μPa (1000 m) ⁻¹)	Francois and Garrison (1982a,b)
β	Spreading loss coefficient	17.5	McQuinn et al. (2011)
v	Ship speed over ground	[5–30] (knot)	From AIS data
l	Ship length	[20–350] (m)	From vessel specification data Lesage et al. (2014)
Simulation duration	Number of simulated days for each simulation replicate	8 (days)	First day of simulation is not considered in analyses (transient time)
Number of belugas	The number of individual belugas generated in each simulation replicate	90	1/10 of the SLE population (to speed up simulations)
Beluga spatial distribution	Spatial distribution of individual belugas across the area	High residency area map	Fig. 1 Lemieux Lefebvre et al. (2012)
Natural background noise	Broadband (0.01–160 kHz) [dB re 1 μPa]	90 (dB re 1 μPa @ 1 m)	Lowest level of natural noise, without human activities Carr et al. (2006)
Scenario	Navigation management measures to which the simulated merchant vessels comply	1) without protection measures; 2) with protection measures	Fig. 1
Period	Time of simulations	25/07–01/08	Busy period for navigation activities in the St. Lawrence

where β is the spreading loss coefficient and $r - r_0$ is the range separating the source from the receiver. Close to the source, spherical spreading dominates and $\beta=20$ (Clay and Medwin, 1998). Farther away, usually at ranges $r - r_0$ corresponding to a few times the height of the water column at the source's position, cylindrical spreading is initiated and $\beta=10$. For long-range hydrophone-assisted observations, both regimes play a role along the source-hydrophone transect and hybrid scenarios are commonly found (i.e., $10 < \beta < 20$).

McQuinn et al. (2011) obtained measurements for β across the St. Lawrence Estuary and the Saguenay Fjord, matching our area of interest. Spatially averaging their results, we obtained a mean spreading loss coefficient of $\beta=17.5$, a value that will be used throughout this work in our calculations of $TL(r_0|r)$.

Water absorption $TL_{abs}(f, r_0|r)$ can be quantified according to:

$$TL_{abs}(f, r_0|r) = \alpha(f) \cdot \left(\frac{r - r_0}{1000 \text{ m}} \right) \quad (12)$$

where the absorption coefficient $\alpha(f)$ is expressed in "attenuation-with-distance" units of dB re 1 μPa (1000 m)⁻¹. Francois and Garrison (1982a,b) provide the formulation for $\alpha(f)$:

$$\alpha(f) = 0.106 \frac{f_1 f^2}{f_1^2 + f^2} \exp\left(\frac{pH - 8}{0.56}\right) + 0.52 \left(1 + \frac{T}{43}\right) \\ \frac{S}{35} \frac{f_2 f^2}{f_2^2 + f^2} \exp\left(\frac{-z}{6}\right) + 4.9 \times 10^{-4} f^2 \exp\left(-\left[\frac{T}{27} + \frac{z}{17}\right]\right) \quad (13)$$

where the frequency f is expressed in kHz, and T , S , z and pH are respectively the temperature (°C), salinity (%), local depth (km), and the relative measure of acidity/alkalinity of the water. The definitions for $f_1 \equiv f_1(S, T)$ and $f_2 \equiv f_2(T)$ are:

$$f_1(S, T) = 0.78 \left(\frac{S}{35} \right)^{\frac{1}{2}} \exp\left(\frac{T}{26}\right) \quad (14a)$$

$$f_2(T) = 42 \exp\left(\frac{T}{17}\right) \quad (14b)$$

Eq. (11) indicates that the individual sound powers in all bands of the source spectrum will be affected identically by geometrical spreading. The dependence on f of Eq. (13), however, shows that absorption of the sound powers will favor a faster attenuation with distance at higher frequencies. Eqs. (11)–(14) were used to

reconstruct the spectrum of received sound levels perceived by a marine mammal by solving for $RL(f, r)$ in Eq. (10) and by adding the non-coherent contributions of all vessels propagating sound within the direct path. Integration along the frequency axis of the resulting spectrum yields the instantaneous broadband sound pressure level sustained by the animal at time step τ_i . The procedure is then repeated for timestep τ_{i+1} for which the residual sound of the previous timestep was judged negligible given our time resolution. Note that a natural background noise level of 90 dB re 1 μPa was added to each broadband measurement retrieved from our model.

2.4. Simulation plan and model outputs

To test the potential impact of the ship strike mitigation measures on the beluga's soundscape, we ran multiple replications of 3MTSim using the set of input parameters (Table 2), for each of the following scenarios:

- 1) Scenario #1: Without the implementation of the protection measures (before 2013). In this scenario, the simulated ship transits statistically reproduce historical patterns (2007).
- 2) Scenario #2: With the protection measures (from 2013 onward). In this scenario, the simulated ship transits comply with the SRA and NGA (cf. Fig. 1).

For each simulation run under scenario #2, we assumed that all merchant ships comply with the voluntary protection measures illustrated in Fig. 1. This means that all ships avoid the NGA and adjust their speed to 10 knots if transiting through the SRA. It is important to mention that we only modelled the noise produced by large merchant and cruise ships in 3MTSim since the ship strike mitigation measures only target these activities. Therefore, the level of noise received by the simulated belugas only account for the contribution of merchant ships in the current version of 3MTSim.

Beluga whales are not distributed evenly throughout their summer critical habitat. Females and calves tend to form distinct groups and tend to avoid groups of adult males (Michaud, 1993). Consequently, we disaggregated our results according to different areas of the beluga's critical habitat, namely the Saguenay River, Upper Estuary, Lower Estuary, and the SRA (Fig. 1). We did so to detect pos-

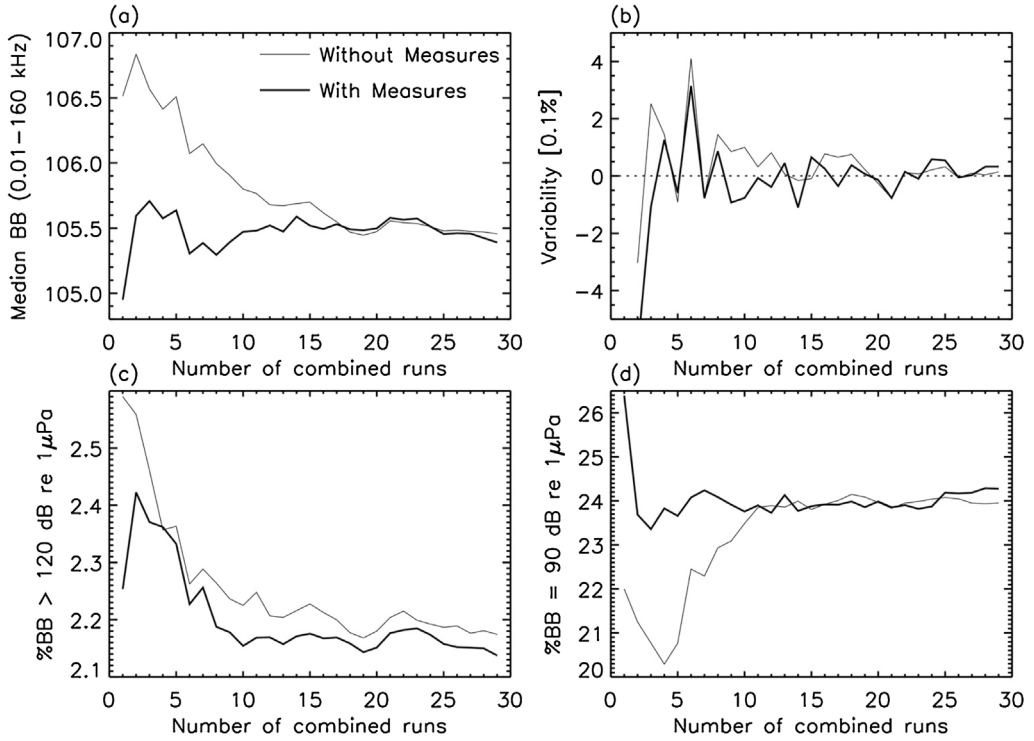


Fig. 5. Panel (a): Median of the broadband levels of noise received by individual belugas as a function of the number of combined simulation runs for the entire computational area (indicator #1). Runs are cumulative in abscissa in the sense that 1 corresponds to the first run only and 29 is the combination of the first 29 runs. To each broadband measurement returned by the 3MTSim simulator, we added 90 dB re 1 μ Pa to account for the natural background noise. This means that the minimal exposure sustained by a beluga at each timestep is 90 dB re 1 μ Pa when the animal is completely isolated from all ships present in the computational area. Panel (b): Relative variation of the median broadband levels (BB) displayed in Panel (a). The variability N_i for a number of stacked runs i is calculated by $N_i = (BB_{i-1} - BB_i)/BB_{i-1} \times 100\%$. Panel (c): Percentage of the number of belugas exposed to an instantaneous broadband noise greater than 120 dB re 1 μ Pa as a function of the number of combined simulation runs (indicator #2). Panel (d): Percentage of the number of belugas exposed to an instantaneous broadband noise equal to the natural background noise of 90 dB re 1 μ Pa as a function of the number of combined simulation runs (indicator #3). In all panels, the thin (thick) line represents runs without (with) management measures.

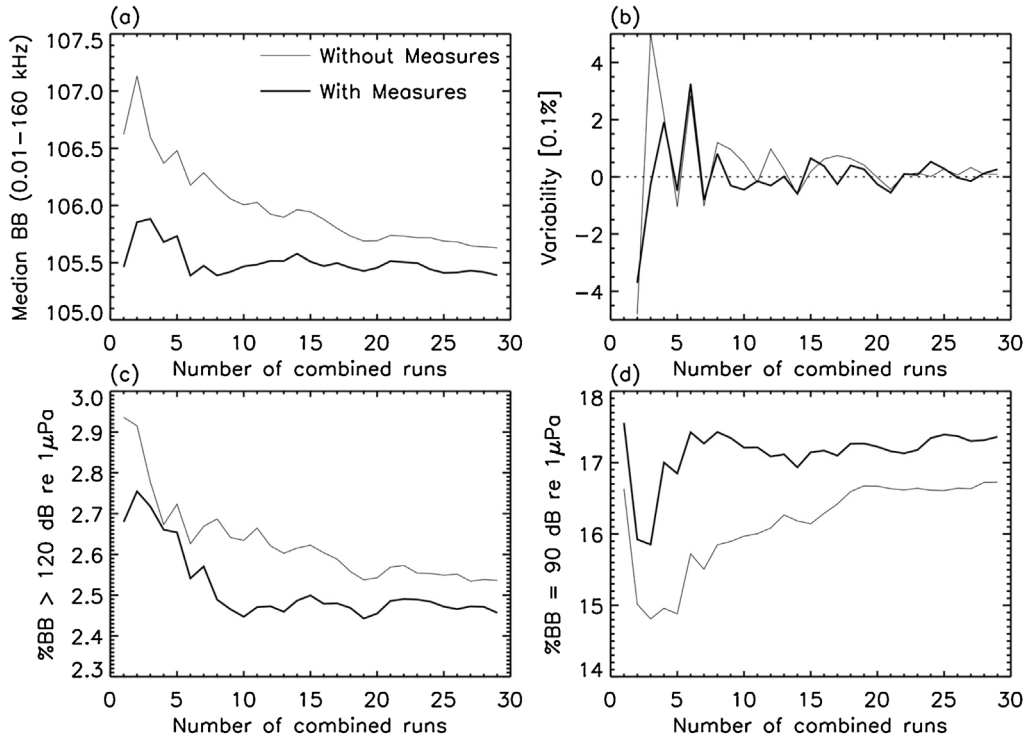


Fig. 6. Same as Fig. 5 for belugas present exclusively in the Upper Estuary.

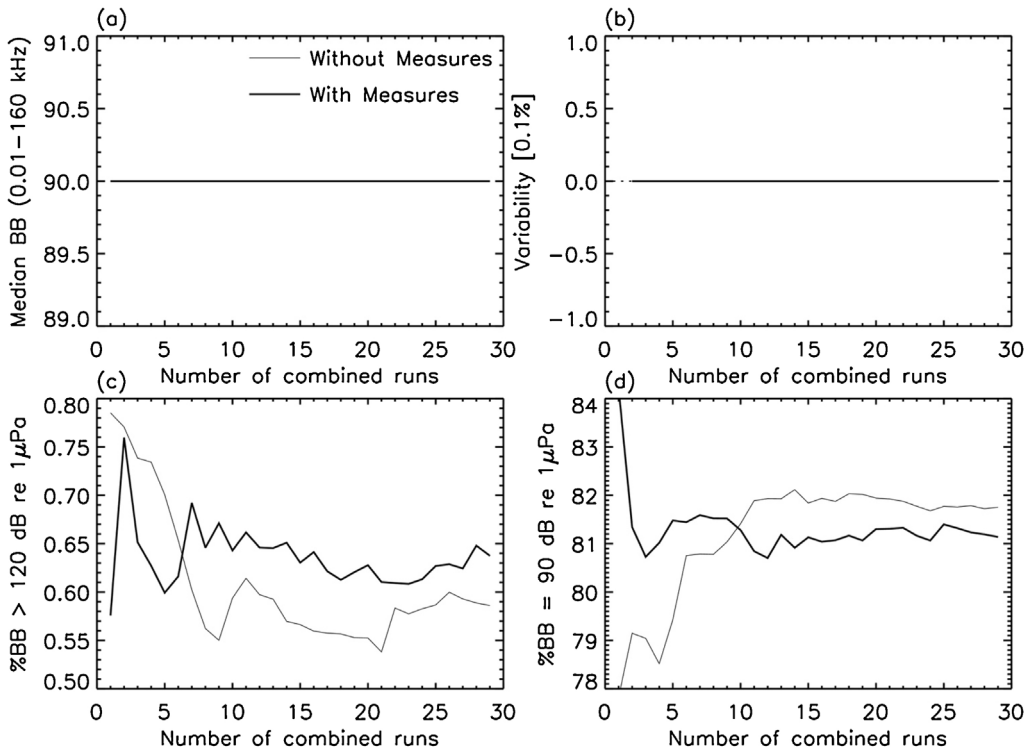


Fig. 7. Same as Fig. 5 for belugas present exclusively in the Saguenay River. The constant plateau at 90 dB re 1 μ Pa is Panel (a) signifies that more than 50% of all animals present in the Saguenay River were isolated from all ships present in the computational area. This is confirmed by the results of Panel (d).

sible spatial variability in the impacts of the protection measures on the soundscape of specific beluga groups.

We used the same series of random seeds for the multiple runs of both scenarios #1 and #2 to control for certain stochastic processes (e.g., initial distribution of belugas) that add noise to the acoustic

phenomena of interest. However, stochasticity also affects several model processes during runtime that may impact the simulated soundscape and add some numerical noise to the results. Such processes include the occurrence of a new ship transit and initial ship characteristics (e.g., length, speed, draught) generated during each

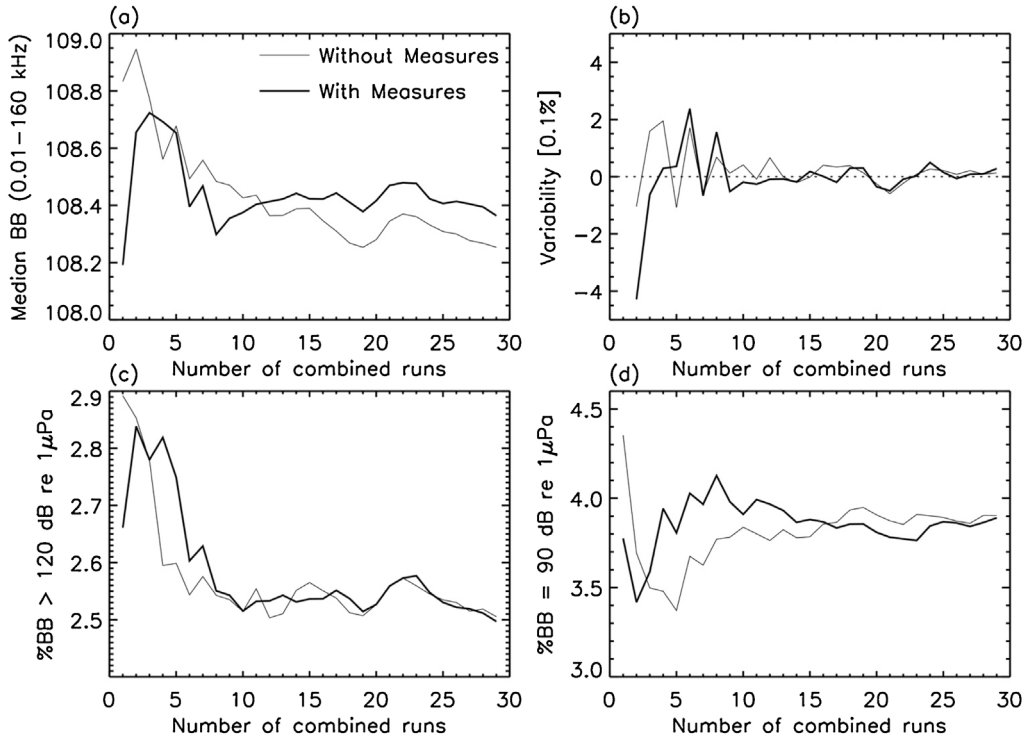


Fig. 8. Same as Fig. 5 for belugas present exclusively in the Lower Estuary.

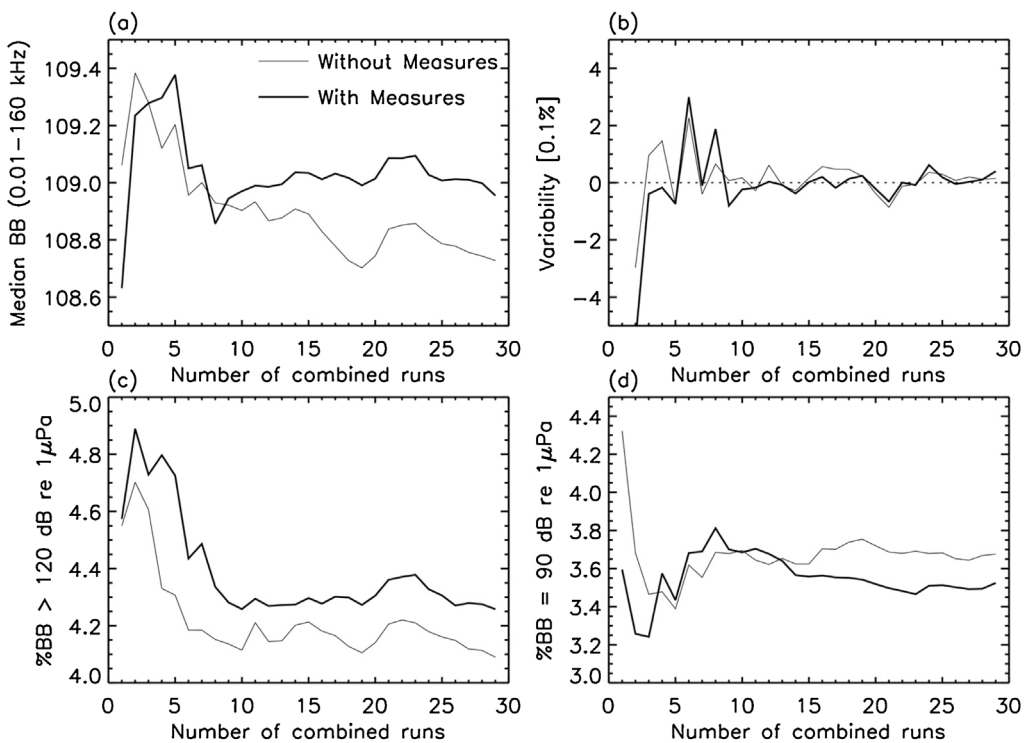


Fig. 9. Same as Fig. 5 for belugas present exclusively in the SRA.

run, determined using a Monte Carlo method (*i.e.*, the generation of initial parameters is randomly drawn from a known probability distribution based on historical data). Stochasticity also occurs within the whale movement model. Consequently, to detect any acoustic variation due to our different scenarios, we ran 29 simulations of 3MTSim until the relative variability between the median broadband levels received by belugas for both scenarios was stable and under 0.1% (Figs. 5–9).

For both scenarios, 3MTSim returns three indicators to detect any acoustic differences in the beluga's soundscape (Table 3). All three indicators are computed from the individual beluga's standpoint. The first acoustic indicator is related to the total amount of merchant ship noise received by individual belugas in their critical habitat and is the median value of these individual received levels. At each time step, each beluga reports the received broadband noise (dB re 1 μ Pa) integrated over the [0.01–160] kHz range. This frequency range spans the entire spectrum of beluga's audio sensitivity (Erbe et al., 2016).

The second acoustic indicator is the percentage of time individual belugas are exposed to more than 120 dB. Sustained evasive actions are observed in some animals (Awbrey and Stewart, 1983).

that can negatively affect beluga whales and other odontocetes (Southall et al., 2008) if exposed above a 120 dB threshold (broadband noise). This threshold of 120 dB of sound pressure level is used for the onset of behavioral harassment of all marine mammals from a continuous source (McQuinn et al., 2011; NOAA, 2016; Weilgart, 2007). Accordingly, this second indicator characterizes the noisiest periods for belugas due to shipping traffic.

Finally, the last indicator is the percentage of time an individual beluga is not exposed to any merchant ship noise. According to the acoustic observations made in one of the quietest area of the SLE (Carr et al., 2006), we set the broadband natural background noise to 90 dB. Although the natural background noise varies in space and time through the SLE (*e.g.*, wind, tides) we decided to take a constant broadband natural background noise as a baseline, which has no influence on the simulated shipping noise we are interested in. Thus, a simulated beluga exposed to only a broadband noise of 90 dB at a given timestep is not receiving any noise from shipping (noise from other fleets is not accounted for in this version of 3MTSim) and therefore is considered to be a quiet period at the beluga's location.

3. Results

Overall, all three acoustic indicators (Table 3) showed small but statistically significant impacts of the protection measures on the belugas' soundscape (Tables 4–6). Throughout the entire beluga habitat, simulations suggest that the protection measures have the potential to reduce the belugas' exposure to broadband noise by 1.6% (linear domain) assuming that all merchant ships comply with the measures in place (Table 4). 3MTSim simulations also suggest that the protection measures decreased the percentage of noisy periods by 1.4% (Table 5) and increased the percentage of quiet periods by 1.4% (Table 6).

The acoustic impacts of the protection measures displayed different patterns of variability within each portion of the beluga's critical habitat. Of the three distinct areas, the Saguenay River is

Table 3
3MTSim acoustic indicators (outputs).

Indicator number	Indicator name	Description
Indicator #1	Median broadband noise received level (dB re 1 μ Pa)	Median of the integrated noise over the range [0.01–160] kHz received by all beluga whales during a simulation
Indicator #2	% noisy periods (>120 dB)	Percentage of time a beluga receives 120 dB (broadband) or more from one or several merchant ships
Indicator #3	% quiet periods (\leq 90 dB = simulated ambient noise)	Percentage of time a beluga is not exposed to any merchant ship

Table 4

Median broadband noise received by belugas from ship transits (indicator #1) broken down by zones (see Fig. 1 to visualize the different zones).

	Median broadband received level (dB re 1 μPa)				
	Upper Estuary	Lower Estuary	Saguenay River	SRA	Study area
(a) Scenario #1: no protection measures	105.63	108.25	90.00	108.73	105.46
(b) Scenario #2: with protection measures	105.39	108.36	90.00	108.96	105.39
(c) Δ %	-5.4%*	+2.6%*	0%	+5.4%*	-1.6%*

* The difference is statistically significant according to the Kolmogorov–Smirnov test ($\alpha = 0.01$).

Table 5

Percentage of noisy periods (indicator #2) broken down by zones (see Fig. 1 to visualize the different zones).

	% of noisy periods – Broadband received levels > 120 dB (dB re 1 μPa)				
	Upper Estuary	Lower Estuary	Saguenay River	SRA	Study area
(a) Scenario #1: no protection measures	2.54%	2.51%	0.59%	4.09%	2.17%
(b) Scenario #2: with protection measures	2.46%	2.50%	0.64%	4.26%	2.14%
(c) Δ % [= (b – a)/a]	-3.1%*	-0.4%*	+8.5%*	+4.2%*	-1.4%*

* The difference is statistically significant according to the Kolmogorov–Smirnov test ($\alpha = 0.01$).

Table 6

Percentage of quiet periods free of shipping noise (indicator #3) broken down by zones (see Fig. 1 to visualize the different zones).

	% of quiet periods – No ship contribution to ambient noise (dB re 1 μPa)				
	Upper Estuary	Lower Estuary	Saguenay River	SRA	Study area
(a) Scenario #1: no protection measures	16.73%	3.90%	81.76%	3.68%	23.95%
(b) Scenario #2: with protection measures	17.36%	3.89%	81.14%	3.52%	24.28%
(c) Δ % [= (b – a)/a]	+3.8%*	-0.3%*	-0.8%*	-4.3%*	+1.4%*

* The difference is statistically significant according to the Kolmogorov–Smirnov test ($\alpha = 0.01$).

the quietest zone for belugas with regards to shipping noise. This excludes the mouth of the Saguenay which is the noisiest portion of the beluga's critical habitat (McQuinn et al., 2011) mainly because of ferries and transits of whale-watching boats, which are not affected by the protection measures and thus are left out of this study. The Lower Estuary is the area where belugas receive the highest level of noise from merchant ships (Fig. 8). The Upper Estuary is quieter than the Lower Estuary with regards to shipping under both scenarios (Table 4). The simulated noise received by belugas in the Upper Estuary is 5.4% lower after the implementation of the protection measures (Table 4), mainly because the noise produced in the SRA by a slower ship extends over shorter distances due to its lower source level. Conversely, in the Lower Estuary where the SRA is located (Fig. 1), simulations showed an increase of 2.6% in the median broadband noise received by belugas in the presence of the protection measures (Table 4), due to slower traffic lengthening the duration of ship transits in the northern channel. This increase in noise exposure reached 5.4% for belugas located within the SRA (Table 4).

With regards to the percentage of quiet periods (Table 6) (i.e., no contribution of local shipping to ambient noise) and the percentage of noisy periods (Table 5) (i.e., the shipping contribution to ambient noise exceeding 120 dB), the trends with and without implementation of the protection measures in each zone are somewhat similar to the median broadband noise indicator (Figs. 5–9). Although there is a positive impact for belugas in the Upper Estuary for these two indicators (Fig. 6a, Tables 5 and 6), there is almost no noticeable change in noisy periods (Table 5) and quiet periods (Table 6) in the Lower Estuary (Fig. 8a).

Finally, the median broadband noise received by belugas in the Saguenay River displays no significant change before vs after the implementation of the protection measures (Fig. 7a). However, the simulations showed an increase of 8.5% (Table 5, Fig. 7c) in the percentage of noisy periods and a decrease of 0.8% (Table 6, Fig. 7d) in the percentage of quiet periods with the protection measures.

4. Discussion

One of the RANDI model assumptions is that the broadband noise produced by a given merchant ship is positively correlated with its speed (through the engine speed). Therefore, a ship is louder at high speed than at low speed. This assumption is supported by evidence from acoustic observations in recent large-scale studies that observed an average decrease of 1 dB/knot (McKenna et al., 2013; Veirs et al., 2016). However, our simulations suggest that speed restrictions lead to a statistically significant increase of 5.4% of the received levels of ship noise by belugas inside the SRA (Table 4). This may appear counter-intuitive since, according to the RANDI model, slower ships should imply a quieter underwater noise budget in the area directly targeted by these speed restrictions. However, although a speed reduction in a given area lowers the instantaneous noise produced by a ship, the net noise emission may be greater since the vessel will take longer to transit through the area, thus insonifying whales over a longer period (McKenna et al., 2013). Therefore, there is a cumulative sound exposure tradeoff to consider when slowing down a ship where whales are present. This tradeoff is illustrated in Appendix B.

The St. Lawrence belugas are gregarious and tend to form pods of different compositions distributed within specific regions of their habitat (Lemieux Lefebvre et al., 2012; Michaud, 1993; Mosnier et al., 2016). In the SLE, females and calves tend to frequent the Upper Estuary whereas males and mixed groups are mostly observed in the Lower Estuary and the Saguenay River (Fig. 10). Consequently, the simulated acoustic impacts of the protection measures presented in this study can be interpreted as mostly beneficial for groups of females and calves that frequent the Upper Estuary (cf. Table 4). This is also reinforced by acoustic observations of female-calf communications that are composed of low energy calls at low frequencies (Vergara and Barrett-Lennard, 2008) easily masked by large ships (Lesage et al., 2014). Considering that females and calves are the most critical members of the population to protect in the context of species at risk recovery, the ship

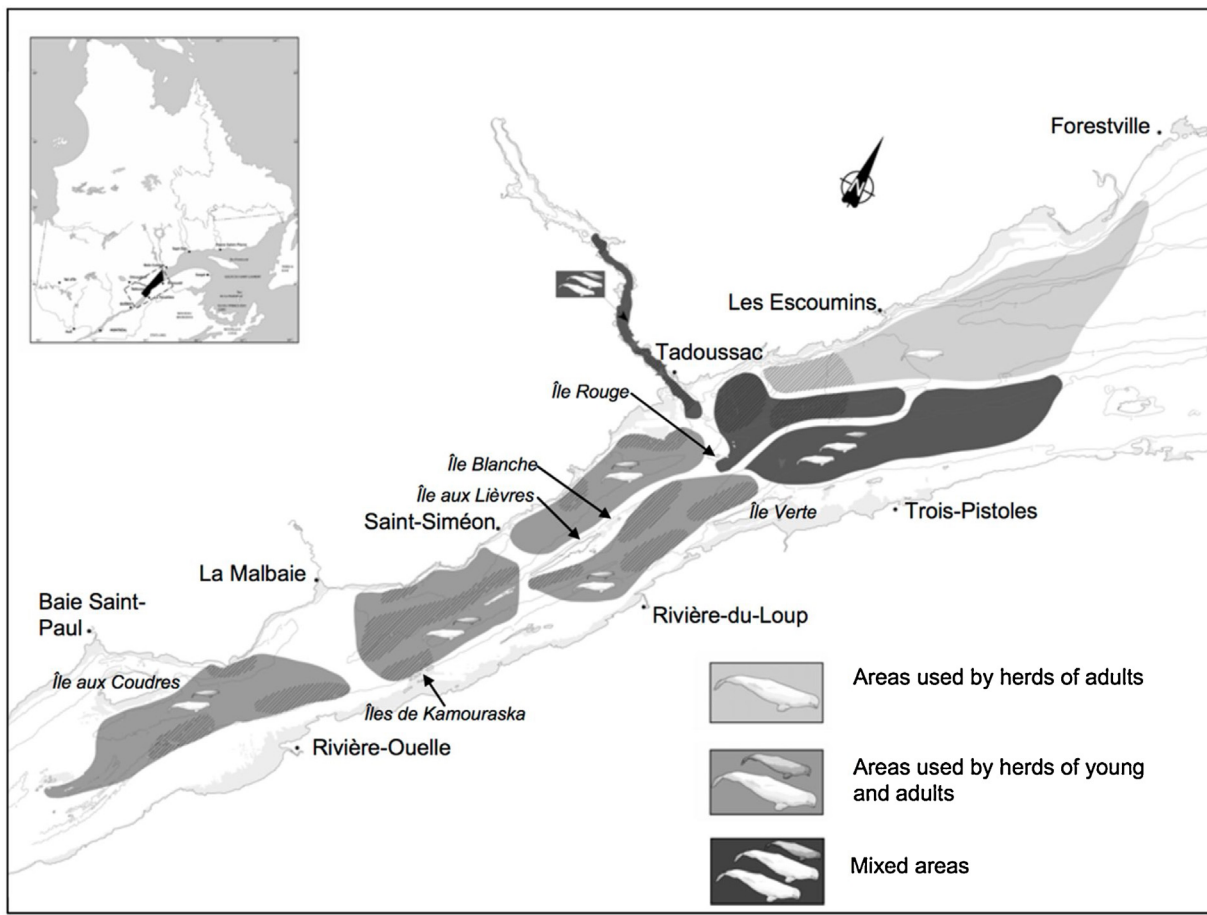


Fig. 10. Distribution of belugas' subgroups across the species' critical habitat (adapted from (Michaud, 1993)).

strike mitigation measures implemented to enhance baleen whale conservation in the SLE appear to be also beneficial in terms of noise reduction in the beluga's habitat mostly frequented by these subgroups (Fig. 10).

Despite the quantitative nature of the results presented in this study, the focus should be put first on the trends and the physical phenomena underlying the statistics since there remain sources of uncertainties not yet quantified. For instance, our adjusted version of RANDI reproduces the trend that a slower ship is less noisy but in a more conservative way (a decrease of 0.22 dB/knot) than some field studies highlight (McKenna et al., 2013; Veirs et al., 2016), meaning that our results possibly underestimate both noise reduction and conservation gains for belugas resulting from ships slowing down in the SRA.

4.1. Implications for management

Through the recently implemented acoustic module in 3MTSim, we have presented the theoretical effects of actual protection measures, *i.e.*, the implementation of speed reduction and no-go areas for merchant ships, on the sound exposure of beluga whales throughout various portions of their critical habitat. In the context of the SLE and the Saguenay River, although speed reduction is an efficient way to mitigate ship strikes, our simulations suggest that it has a more limited impact on decreasing shipping noise from merchant ships at the scale of the entire beluga critical habitat. However, this management tool now has the potential to investigate many other marine traffic-marine mammal interaction scenarios and the impacts these potential changes would have on the soundscape within the SLE such as modifications to

the fleet composition or rerouting of traffic lanes which would be very difficult to implement and measure in the field. Further, 3MTSim could be used to assess the impact of regulations pertaining to whale-watching boats, ferries and pleasure craft on the beluga's soundscape which has the potential of greater effects than presented here given their much larger number of trips and closer proximity to sensitive beluga habitat (McQuinn et al., 2011).

There is also a need to better identify the critical communication frequencies used by belugas for their vital activities to better design noise mitigation solutions. It is crucial to determine whether a longer exposure to lower noise is better or worse than a shorter exposure to louder noise, as this will help determine which traffic management measures might be the most effective in reducing noise impacts on beluga. Identifying noise thresholds at critical frequencies may help in designing efficient mitigation measures, including soundproofing engineering solutions at the shipbuilding stage along with the maintenance or retrofit of ship hulls and propellers (Hemera Envirochem Inc, 2016). As part of an adaptive management process, the Working Group will continue to use the best information available to make recommendations that seek to reduce collision risks while also reducing noise in the belugas' soundscape. The acoustic additions to 3MTSim along with further developments will make it a valuable tool to inform this process.

4.2. Future work

3MTSim will continue to be refined to improve the accuracy of the simulated soundscape and to investigate potential impacts on marine mammals. First, the prediction accuracy of source levels from ships derived from the RANDI model can be refined by

increasing the number of ship noise signatures used for parameterization. Particularly, the relationship between ship speed and noise signature can be better characterized. Regardless of these improvements, we are aware that modelling ship noise with RANDI through such inputs as speed, length and draught has limitations since other attributes not available in AIS data may also have impacts on noise emission (e.g., propeller condition, cargo loading). Consequently, using additional ship sound signatures to adjust RANDI would increase its accuracy by assessing the confidence intervals of 3MTSim outputs.

Improvements can also be made to the sound propagation modelling in the complex environment of the SLE and the Saguenay River. Although we used a simple geometrical spreading model parameterized specifically for the study area (McQuinn et al., 2011), sound propagation is affected by environmental factors other than bathymetry which may vary throughout the belugas' habitat. For instance, the water column can be stratified in parts of the study area, generating sound channeling effects. Although these effects were generally accounted for in the current version of the model by using empirically-derived transmission loss coefficients, there are tidally modulated spatial and temporal components that could affect our results. Another influential physical attribute of the environment is the seafloor composition that is responsible for the reflection and absorption of sound. Using advanced propagation models such as RAM based on parabolic equations could improve modelling results (Farcas et al., 2016), particularly in the Saguenay River where steep-sided underwater cliffs are known to increase the resonance (McQuinn et al., 2011).

Finally, another series of improvements can be made to the modelling of the beluga's behavioural response to anthropogenic noise. Observations made in the area revealed that belugas tend to modify their acoustic behaviors to overcome the presence of background noise, known as the Lombard effect (Lesage et al., 1999). However, there remain knowledge gaps on the short- to long-term impacts of masking on belugas acoustic activities. For instance, the disruption of mother-calf contact calls by anthropogenic noise could be related to the increased number of abandoned live calves or carcasses found every year in the SLE. An important improvement to 3MTSim would be to incorporate frequency weighting to account for the hearing capacity of beluga and other marine mammals [*sensu* (McQuinn et al., 2011)]. This would affect species-specific sound exposure estimates as well as the estimated potential for masking.

We showed that combining agent-based modelling with acoustic modelling has the potential to inform the conservation of endangered whale populations by facilitating the design and test of spatial and temporal mitigation measures including seasonal ship-speed and route restrictions. If additional acoustic data become available, they may be incorporated into the acoustic module of 3MTSim and further improve our ability to identify zones of acoustic sensitivity. Such noise mitigation options as the conservation or addition of acoustic refuges (Williams et al., 2015) in ecologically sensitive areas could also be tested to quantify their acoustic impacts on the St Lawrence beluga's critical habitat.

5. Conclusion

The disturbance of marine mammals by human activities is multidimensional and species-specific. Accordingly, there is a need for conservation tools that can project how different risks induced by human activities on different marine mammal species evolve under alternative management scenarios. In this context, we used 3MTSim to assess the acoustic impacts on belugas of recently implemented protection measures designed to mitigate the risk of collisions between ships and baleen whales in the SLE. The main

simulation results revealed the potential of the ship strike mitigation measures to reduce belugas' exposure to shipping noise, the greatest benefits being in areas frequented by females and calves. The beluga population being listed as endangered species according to the Canadian Species at Risk Act, the protection of females and calves is a priority from a recovery perspective. However, 3MTSim revealed that the acoustic impacts of the voluntary protection measures varied spatially, with the belugas located close to the SRA being more exposed to shipping noise because ships travelling slower are staying longer in that area. This highlights the existence of a critical distance above which the total contribution to underwater noise of a ship at low speed (*i.e.*, longer insonification) exceeds its total contribution at a higher speed (*i.e.*, higher instantaneous noise); physical properties such as sound spreading loss, absorption, and the frequency-dependence of sound propagation support this observation.

3MTSim highlighted a fundamental difference between the mitigation of ship strike risks and noise reduction in a given area frequented by whales. Whereas slowing down merchant ships decreases the local risks of lethal ship strikes (Vanderlaan and Taggart, 2007), it likely increases the total amount of acoustic energy released locally (McKenna et al., 2013). Therefore, fine-scale knowledge of the species-specific and frequency-dependent acoustic thresholds above which ecological impacts are observed must be acquired to inform the design of mitigation measures using acoustic impact assessment tools such as 3MTSim.

Acknowledgments

Funding for this project was provided by the MEOPAR, a member of the Canadian Networks of Centres of Excellence. This publication draws on Satellite AIS data which are provided by exactEarth Ltd. 2016, and processed courtesy of MEOPAR.

Appendix A. Changes in ship speed across the study area since the implementation of the protection measures

Since the implementation of the voluntary protection measures in 2013, the maritime industry has shown significant changes in their operations, mostly by slowing down in the SRA (cf. Fig. A1d). Fig. A1 shows that the measures had no significant impacts on ship speed outside of the Lower Estuary with the greatest speed reduction occurring in the SRA.

The statistically significant reduction in ship speed in the Lower Estuary excluding the SRA after vs. before the implementation of the protection measures (Fig. A1e) indicates that there is a positive side-effect of the protection measures that extend beyond their boundaries.

Appendix B. Ecological tradeoff between fast and noisy vs slow and quieter ships

To illustrate the ecological tradeoff, we propose a simple model (Fig. B1). A 500×100 km² computational area is created with a spatial resolution of 1 km pixel⁻¹. Two ships are modeled separately, hence two distinct simulations were carried out. Ship A is not restricted by any speed limitations and travels at 20 knots, a speed that we defined as 2 pixels per timestep (or 2 km per timestep). This itself defines our timestep τ at 194.3 s. Alternatively, Ship B is speed-restricted and travels at 10 knots *i.e.*, 1 pixel per timestep (or 1 km per timestep). Both ships move horizontally along the lower abscissa in Panel (a). Along the imaginary vertical line above the origin are positioned 100 beluga whales, each spaced by 1 km. The belugas are motionless and simply act as noise receivers at their respective position.

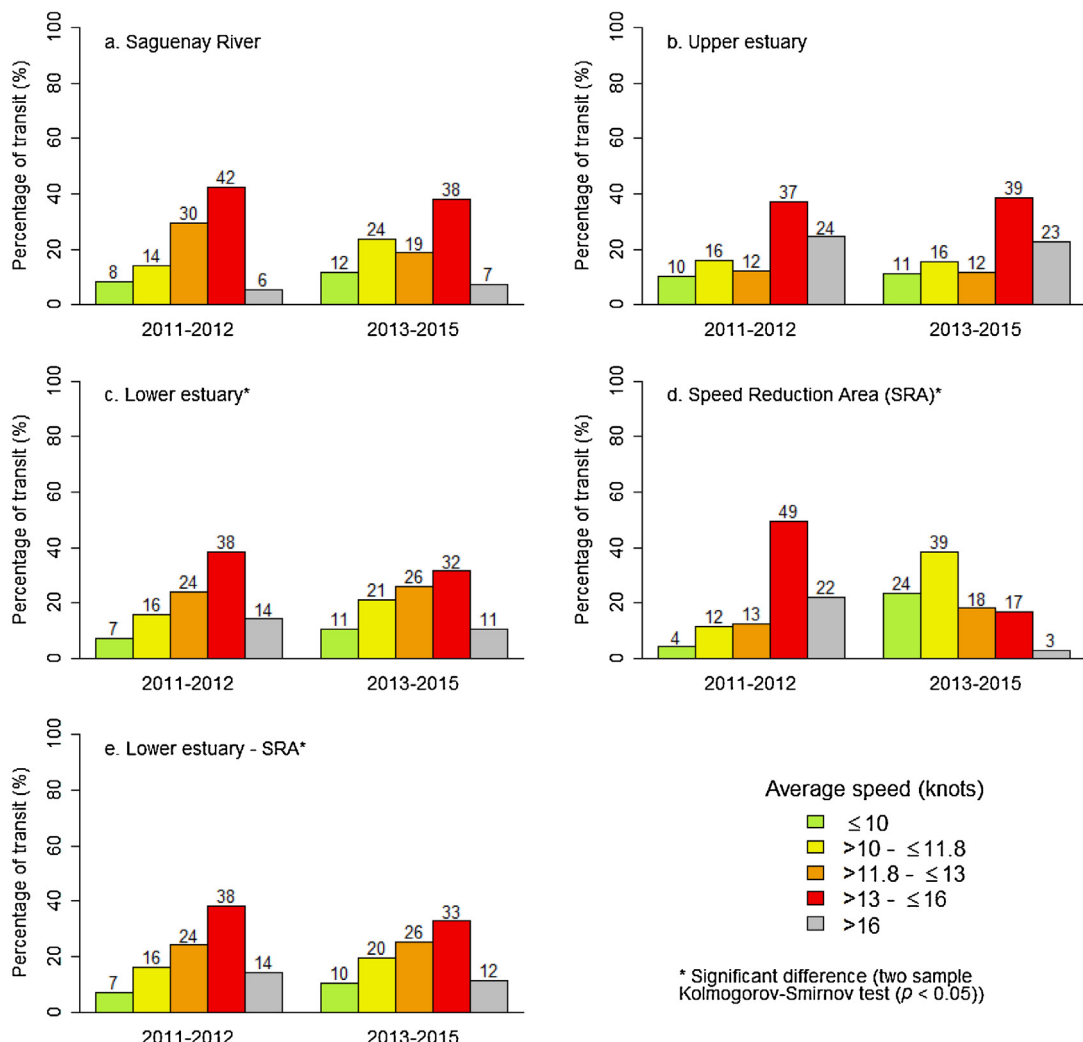


Fig. A1. Changes in ship-speed patterns before (2011–2012) and after (2013–2015) the implementation of the voluntary protection measures. The difference between speed distributions is: Panel (a) – not statistically significant ($\alpha = 0.05$) in the Saguenay River ($p\text{-value} = 0.085$, Kolmogorov-Smirnov test); Panel (b) – not statistically significant ($p\text{-value} = 0.146$); Panel (c) – statistically significant ($p\text{-value} < 2.2 \times 10^{-16}$) in the Lower Estuary; Panel (d) – statistically significant in the SRA ($p\text{-value} < 2.2 \times 10^{-16}$); Panel (e) – statistically significant in the Lower Estuary excluding the SRA ($p\text{-value} < 2.2 \times 10^{-16}$). (AIS data sources: Parks Canada; exactEarth inc.).

Using Eq. (9), broadband noise levels at the source were estimated at 184.11 and 182.40 dB re 1 μPa @ 1 m for Ships A and B, respectively. Considering a natural background noise level of 90 dB re 1 μPa and using the theory for sound propagation described earlier, we estimated, for each ship, the range at which the broadband received level precisely matches this value. This corresponds to the distance beyond which each ship clearly becomes indistinguishable from the natural background noise. These distances are respectively estimated at 240 and 190 km for Ships A and B and correspond in Fig. B1a to the starting point of each ship with respect to the diagram's origin (the origin corresponds to the position occupied by Beluga #0). To obtain the whole noise budget for each ship, Ship A will travel from left to right between –240 and +240 km along the lower abscissa. Considering a traveling speed of 2 pixels per timestep and our spatial resolution of 1 km pixel $^{-1}$ (see above), 240 timesteps will therefore be required for Ship A to cover the appropriate distance. Similarly, Ship B will have a trajectory between –190 and +190 km and, for a traveling speed of 1 pixel per timestep (see above), and 380 timesteps will be required. End points for both ships are shown near the abscissa's right-hand extremity (Fig. B1a). At each timestep, broadband received levels are measured at the

positions occupied by each of the 100 beluga whales stacked above the origin (Fig. B1a).

Following the transit of Ship A, 240 broadband measurements will have been recorded for each of the 100 belugas i.e., one measurement for each of the 240 timesteps required for Ship A to cover the required distance. Similarly, for Ship B, 380 measurements will have been obtained for each whale. The median broadband level is then computed for each receiver. The results for all 100 receivers, each occupying a 1 km linear volume, are displayed for both ships in Fig. B1b. Although Ship B is quieter at the source, the fact that it spends more time in the direct vicinity of the diagram's origin in Fig. B1a leads to received noise levels exceeding the ones of the faster ship who spends half the amount of time (when compared to Ship B) near (0,0). This behavior, however, is only observed for a certain radial distance away from the traveling axis. The noisier Ship A eventually dominates the noise budget at radial distances exceeding 21 km from the lower abscissa (Fig. B1b). This demonstrates the existence of a critical distance inside which speed restrictions could lead to a localized negative effect in terms of received noise levels. This may explain the increase by 5.4% in broadband measurements obtained in the SRA while, far beyond the critical distance, speed restrictions result in a quieter environment in the Upper Estuary.

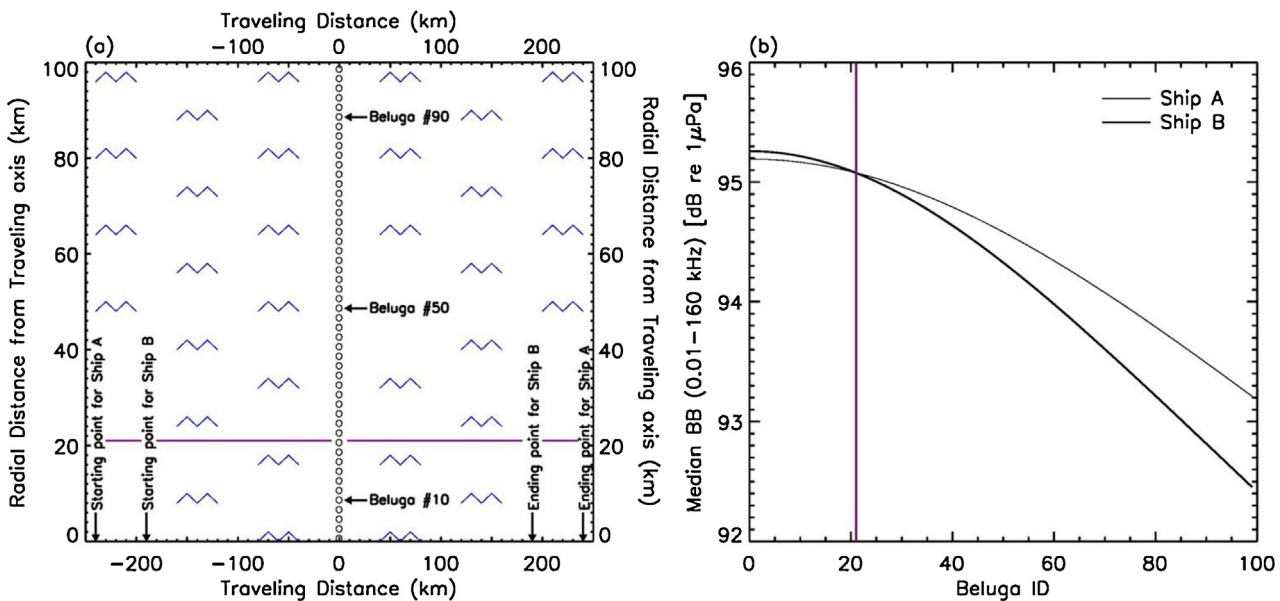


Fig. B1. Panel (a): Experimental set up to illustrate the notion of a critical distance inside which ship speed restrictions lead to an increase of the noise levels received by belugas. This panel must be interpreted as a $500 \times 100 \text{ km}^2$ body of water seen from above. Ships A and B travel from left to right (starting and ending points for each ship are identified). Both ships measure 250 m in length. The water temperature, salinity, depth, and pH were respectively fixed at 10°C , 35‰, 100 m, and 8 in our calculation of the absorption coefficient $\alpha(f)$ provided by Eq. (13). Beluga whales (receivers) are aligned along the imaginary vertical line above the (0,0)-origin and are symbolized by open circles. For clarity, only 1 out of 2 beluga whales are displayed. Panel (b): Median broadband noise levels received by each beluga whale following the passage of Ships A (thin line) and B (thick line) respectively. In both panels, the purple line indicates the critical distance. Inside this distance, the quieter-at-the-source Ship B is responsible for higher received noise levels. Beyond the purple line, the noisier Ship A dominates the noise budget (see text for details).

Let us note that the critical distance is dependent on our model of ship source level. Since the RANDI-adjusted model is likely underestimating noise reduction with ship speed reduction, the actual critical distance may be shorter than illustrated here.

References

- ANSI, 2009. Quantities and Procedures for Description and Measurements of Underwater Sound from Ships—Part 1: General Requirements, Accredited Standards Committee S12. Acoustical Society of America Standards Secretariat, NY.
- Arveson, P.T., Vendittis, D.J., 2000. Radiated noise characteristics of a modern cargo ship. *J. Acoust. Soc. Am.* 107, 118–129.
- Awbrey, F.T., Stewart, B.S., 1983. Behavioral responses of wild beluga whales (*Delphinapterus leucas*) to noise from oil drilling. *J. Acoust. Soc. Am.* 74, S54–S54.
- Bassett, C., Polagye, B., Holt, M., Thomson, J., 2012. A vessel noise budget for Admiralty Inlet, Puget Sound, Washington (USA). *J. Acoust. Soc. Am.* 132, 3706–3719.
- Beauchamp, J., Bouchard, H., de Margerie, P., Otis, P., Savaria, J.-Y., 2009. Recovery Strategy for the Blue Whale (*Balaenoptera Musculus*), Northwest Atlantic Population, in Canada [FINAL]. Species at Risk Act (SARA) Recovery Strategy Series. Fisheries and Oceans Canada, Ottawa.
- Bonabeau, E., 2002. Agent-based modeling: methods and techniques for simulating human systems. *Proc. Natl. Acad. Sci. U. S. A.* 99, 7280–7287.
- Breeding Jr., J.E., Pflug, L.A., Bradley, M., Walrod, M.H., 1996. Research Ambient Noise Directionality (RANDI) 3.1 Physics Description.DTIC Document.
- Canadian Coast Guard, 2016. Notices to Mariners Publication – Eastern Edition.
- Carr, S.A., Laurinolli, M.H., Tollesfson, C.D.S., Turner, S.P., 2006. *Cacouna Energy LNG Terminal: Assessment of Underwater Noise Impacts*. JASCO Research Ltd.
- Chion, C., Turgeon, S., Michaud, R., Landry, J.-A., Parrott, L., 2009. *Portrait de la Navigation dans le Parc Marin du Saguenay-Saint-Laurent. Caractérisation des activités sans prélevement de ressources entre le 1er mai et le 31 octobre 2007*. École de technologie supérieure/Université de Montréal.
- Chion, C., Lamontagne, P., Turgeon, S., Parrott, L., Landry, J.-A., Marceau, D.J., Martins, C.C.A., Michaud, R., Ménard, N., Cantin, G., et al., 2011. Eliciting cognitive processes underlying patterns of human-wildlife interactions for agent-based modelling. *Ecol. Model.* 222, 2213.
- Chion, C., Parrott, L., Landry, J.-A., 2012. Collisions et cooccurrences entre navires marchands et baleines dans l'estuaire du Saint-Laurent—Évaluation de scénarios de mitigation et recommandations. Université de Montréal.
- Chion, C., Cantin, G., Dionne, S., Dubeau, B., Lamontagne, P., Landry, J.-A., Marceau, D., Martins, C.C., Ménard, N., Michaud, R., 2013. Spatiotemporal modelling for policy analysis: application to sustainable management of whale-watching activities. *Mar. Policy* 38, 151–162.
- Chion, C., Landry, J.-A., Parrott, L., Marceau, D.J., Lamontagne, P., Turgeon, S., Michaud, R., Martins, C.C., Ménard, N., Cantin, G., Dionne, S., 2014. In: Higham, J., Bejder, L., Williams, R. (Eds.), *Insights from Agent-Based Modelling to Simulate Whale-Watching Tours*.
- Chion, C., 2011. *An Agent-based Model for the Sustainable Management of Navigation Activities in the Saint Lawrence Estuary* (Doctoral Thesis). École de technologie supérieure, Montréal (Canada).
- Chion, C., 2016. Réduction des risques de collisions mortelles de grands rorquals avec des navires marchands dans l'estuaire du Saint-Laurent en 2015 (Scientific Report). Université du Québec en Outaouais, Gatineau (QC).
- Clay, C.S., Medwin, H., 1998. *Fundamentals of Acoustical Oceanography (Applications of Modern Acoustics)*. Academic Press.
- Erbe, C., MacGillivray, A., Williams, R., 2012. Mapping cumulative noise from shipping to inform marine spatial planning. *J. Acoust. Soc. Am.* 132, EL423–EL428.
- Erbe, C., Reichmuth, C., Cunningham, K., Lucke, K., Dooling, R., 2016. Communication masking in marine mammals: a review and research strategy. *Mar. Pollut. Bull.* 103, 15–38.
- Farcas, A., Thompson, P.M., Merchant, N.D., 2016. Underwater noise modelling for environmental impact assessment. *Environ. Impact Assess. Rev.* 57, 114–122.
- Finneran, J.J., Schlundt, C.E., Dear, R., Carder, D.A., Ridgway, S.H., 2002. Temporary shift in masked hearing thresholds in odontocetes after exposure to single underwater impulses from a seismic watergun. *J. Acoust. Soc. Am.* 111, 2929–2940.
- Fisheries and Oceans Canada, 2012. Recovery Strategy for the Beluga (*Delphinapterus Leucas*) St. Lawrence Estuary Population in Canada, Species at Risk Act (SARA) Recovery Strategy Series. Fisheries and Oceans Canada, Ottawa.
- Francois, R.E., Garrison, G.R., 1982a. Sound absorption based on ocean measurements. Part II: boric acid contribution and equation for total absorption. *J. Acoust. Soc. Am.* 72, 1879–1890.
- Francois, R.E., Garrison, G.R., 1982b. Sound absorption based on ocean measurements. Part I: pure water and magnesium sulfate contributions. *J. Acoust. Soc. Am.* 72, 896–907.
- Gomez, C., Lawson, J.W., Wright, A.J., Buren, A.D., Tollit, D., Lesage, V., 2016. A systematic review on the behavioural responses of wild marine mammals to noise: the disparity between science and policy. *Can. J. Zool.* 94, 801–819, <http://dx.doi.org/10.1139/cjz-2016-0098>.
- Government of Canada, 1997. *Saguenay-St. Lawrence Marine Park Act*.
- Grimm, V., Revilla, E., Berger, U., Jeltsch, F., Mooij, W.M., Railsback, S.F., Thulke, H.-H., Weiner, J., Wiegand, T., DeAngelis, D.L., 2005. *Pattern-oriented modeling of agent-based complex systems: lessons from ecology*. *Science* 310, 987–991.
- Hemmera Envirochem Inc., 2016. Vessel Quieting Design, Technology, and Maintenance Options for Potential Inclusion in EcoAction Program Enhancing Cetacean Habitat and Observation Program (No. 302-045.03). Burnaby (BC).
- Lair, S., Measures, L.N., Martineau, D., 2012. Pathologic findings and trends in mortality in the beluga (*Delphinapterus leucas*) population of the St Lawrence Estuary, Quebec, Canada, From 1983 to 2012. *Vet. Pathol.* 53 (1), 22–36.

- Laist, D.W., Knowlton, A.R., Mead, J.G., Collet, A.S., Podesta, M., 2001. Collisions between ships and whales. *Mar. Mamm. Sci.* 17, 35–75, <http://dx.doi.org/10.1111/j.1748-7692.2001.tb00980.x>.
- Lamontagne, P., 2009. Modélisation spatio-temporelle orientée par patrons avec une approche basée sur individus.
- Lemieux Lefebvre, S., Michaud, R., Lesage, V., Berteaux, D., 2012. Identifying high residency areas of the threatened St. Lawrence beluga whale from fine-scale movements of individuals and coarse-scale movements of herds. *Mar. Ecol. Prog. Ser.* 450, 243–257.
- Lesage, V., Barrette, C., Kingsley, M., Sjare, B., 1999. The effect of vessel noise on the vocal behavior of belugas in the St. Lawrence River estuary, Canada. *Mar. Mamm. Sci.* 15, 65–84.
- Lesage, V., McQuinn, I., Carrier, D., Gosselin, J.-F., Mosnier, A., 2014. Exposure of the Beluga (*Delphinapterus Leucas*) to Marine Traffic Under Various Scenarios of Transit Route Diversion in the St. Lawrence Estuary (No. 2013/125), DFO – Canadian Science Advisory Secretariat. Fisheries and Oceans Canada, Ottawa.
- McKenna, M.F., Ross, D., Wiggins, S.M., Hildebrand, J.A., 2012. Underwater radiated noise from modern commercial ships. *J. Acoust. Soc. Am.* 131, 92–103.
- McKenna, M.F., Wiggins, S.M., Hildebrand, J.A., 2013. Relationship between container ship underwater noise levels and ship design, operational and oceanographic conditions. *Sci. Rep.* 3.
- McQuinn, I.H., Lesage, V., Carrier, D., Larrivée, G., Samson, Y., Chartrand, S., Michaud, R., Theriault, J., 2011. A threatened beluga (*Delphinapterus leucas*) population in the traffic lane: vessel-generated noise characteristics of the Saguenay-St. Lawrence Marine Park. *Canada. J. Acoust. Soc. Am.* 130, 3661, <http://dx.doi.org/10.1121/1.3658449>.
- Michaud, R., Giard, J., 1997. Les rorquals communs et les activités d'observation en mer dans l'estuaire du Saint-Laurent entre 1994 et 1996: (1) Étude de l'utilisation du territoire et évaluation de l'exposition aux activités d'observation à l'aide de la télémétrie VHF. Group for Research and Education on Marine Mammals (GREMM), Tadoussac (Canada).
- Michaud, R., Bédard, C., Mingelbier, M., Gilber, M.-C., 1997a. *Whale Watching Activities at Sea in the St. Lawrence Marine Estuary, 1985–1996: A Study of Spatial Distribution of Activities and Factors Favouring Boat Aggregation at Whale-watching Sites*. Group for Research and Education on Marine Mammals (GREMM), Tadoussac (Canada).
- Michaud, R., Bédard, C., Mingelbier, M., Gilbert, M.-C., 1997b. *Whale Watching Activities at Sea in the St. Lawrence Marine Estuary 1985–1996: A Study of Spatial Distribution of Activities and Factors Favouring Boat Aggregation at Whale Watching Sites*. Group for Research and Education on Marine Mammals (GREMM), Tadoussac (Canada).
- Michaud, R., D'Arcy, M.-H., de la Chenelière, V., Moisan, M., 2008. *Les activités d'observation en mer (AOM) dans l'estuaire du Saint-Laurent: Zone de Protection Marine Estuaire du Saint-Laurent et Parc Marin du Saguenay-Saint-Laurent-Suivi annuel 2007*. Group for Research and Education on Marine Mammals (GREMM), Tadoussac (Canada).
- Michaud, R., 1993. Distribution estivale du béluga du Saint-Laurent: synthèse 1986 à 1992 (No. 1906). In: *Can. Tech. Rep. Fish. Aquat. Sci. GREMM*.
- Mosnier, A., Larocque, R., Lebeuf, M., Gosselin, J.-F., Dubé, S., Lapointe, V., Lessage, V., Lefebvre, D., Senneville, S., Chion, C., 2016. Définition et caractérisation de l'habitat du béluga (*Delphinapterus leucas*) de l'estuaire du Saint-Laurent selon une approche écosystémique. (No. 2016/052), DFO – Canadian Science Advisory Secretariat. Fisheries and Oceans Canada, Mont-Joli. (QC, Canada).
- NOAA, 2016. *Ocean Noise Strategy Roadmap*.
- Parks Canada, 2002. *Marine Activities in the Saguenay-St Lawrence Marine Park Regulations*.
- Parrott, L., Chion, C., Martins, C.C.A., Lamontagne, P., Turgeon, S., Landry, J.-A., Zhens, B., Marceau, D.J., Michaud, R., Cantin, G., 2011. A decision support system to assist the sustainable management of navigation activities in the St. Lawrence River Estuary, Canada. *Environ. Model. Softw.* 26, 1403–1418.
- Parrott, L., Chion, C., Turgeon, S., Ménard, N., Cantin, G., Michaud, R., 2016. Slow down and save the whales. *Solut. J.* 6, 40–47.
- Ross, D., 1987. *Mechanics of Underwater Noise*. Peninsula Publishing, Los Altos (CA).
- Schlundt, C.E., Finnegan, J.J., Carder, D.A., Ridgway, S.H., 2000. Temporary shift in masked hearing thresholds of bottlenose dolphins and white whales after exposure to intense tones. *J. Acoust. Soc. Am.* 107, 3496–3508.
- Southall, Brandon L., Bowles, Ann E., Ellison, William T., Finneman, James J., Gentry, Roger L., Greene Jr., Charles R., Kastak, David, Ketten, Darlene R., Miller, James H., Nachtigall, Paul E., Richardson, W. John, Thomas, Jeanette A., Tyack, Peter L., 2008. *Marine mammal noise-exposure criteria: initial scientific recommendations*. *Bioacoustics* 17 (1–3), 273–275.
- Species at Risk Act (Canada), 2002.
- Vanderlaan, A.S.M., Taggart, C.T., 2007. Vessel collisions with whales: the probability of lethal injury based on vessel speed. *Mar. Mammal Sci.* 23, 144–156.
- Veirs, S., Veirs, V., Wood, J.D., 2016. Ship noise extends to frequencies used for echolocation by endangered killer whales. *PeerJ* 4, e1657.
- Vergara, V., Barrett-Lennard, L.G., 2008. Vocal development in a beluga calf (*Delphinapterus leucas*). *Aquat. Mamm.* 34, 123.
- Weilgart, L.S., 2007. The impacts of anthropogenic ocean noise on cetaceans and implications for management. *Can. J. Zool.* 85, 1091–1116.
- Williams, R., Erbe, C., Ashe, E., Clark, C.W., 2015. Quiet (er) marine protected areas. *Mar. Pollut. Bull.* 100, 154–161.